Highly Efficient Triplet Chain Isomerization of Dewar Benzenes: Adiabatic Rate Constants from Cage Kinetics

Paul B. Merkel,*,† Yeonsuk Roh,† Joseph P. Dinnocenzo,*,† Douglas R. Robello,‡ and Samir Farid*,†

Department of Chemistry and the Center for Photoinduced Charge Transfer, University of Rochester, Rochester, New York 14627-0216, and Research Laboratories, Eastman Kodak Company, Rochester, New York 14650-2116

Received: November 12, 2006

Quantum yields as high as 120 were achieved for triplet-sensitized photoisomerizations of several Dewar benzene reactants, R, to the corresponding benzene products, P. Considerable chain amplification is maintained even at high conversion. All relevant rate constants of this triplet chain reaction were extracted from laser flash photolysis plus steady-state photolysis experiments. The crucial rate constant k_a for adiabatic isomerization of the triplet reactant to triplet product (R* → P*) cannot be directly measured because it is so large relative to the bimolecular rate of R* formation via sensitization. However, k_a was obtained indirectly using a cage/encounter complex model to analyze the competition between the dissociation of encounter pairs with the sensitizer, e.g., S/R* → S + R*, and the in-cage processes, S/R* → S/P* → S*/P, in nonviscous and viscous solvents. These measurements yielded k_a values of $(\sim 4-9) \times 10^9$ s^{-1}, which suggests that only a small (~3 kcal/mol) energy barrier exists along the potential energy surface from R* to P*. Steady-state data indicated that the chain-terminating rate constant R* → R is negligibly small, an ideal condition for chain amplification. Triplet energy transfer from a series of sensitizers to the Dewar benzene derivatives shows a nonclassical falloff in rate constants with decreasing sensitizer triplet energy, suggesting energy transfer to thermally distorted configurations having lower singlet−triplet energy gaps. As a result of distorted geometries of R* and P*, the chain-propagating energy transfer from P* to R proceeds with a rate constant of only $\sim 2 \times 10^7$ M^{-1} s^{-1}, despite strong exothermicity. The isomerization reaction can release over 100 kcal/kcal of absorbed photons due to the high-energy content of the reactant together with the large chain length.

Introduction

A new class of photoresponsive materials has recently been described utilizing a process called quantum amplified isomerization (QAI).[1] These QAI materials are based on photoinitiated electron-transfer chain isomerization reactions that alter the properties of a polymer matrix. When the QAI reactions result in large changes in the refractive index, the materials have been shown to have potential applications for optical recording.[1b] Thus far, QAI materials have displayed only moderate photosensitivities, limiting their practical applications. A key disadvantage of these materials is that chain amplification requires charge separation of the intermediate radical ion pairs that are generated by photoinduced electron transfer. The Coulombic barrier for charge separation is significant in nonpolar polymer matrixes, favoring instead chain-terminating return electron transfer. A QAI chain reaction based on *energy transfer* instead of electron transfer would eliminate the restrictions to chain propagation imposed by the Coulombic barrier and potentially lead to more efficient materials.

A number of examples of chain isomerization processes that proceed via triplet-excited-state intermediates have been previously reported,[2−4] some with reasonable efficiencies. For example, quantum yields as high as ~40 have been measured for sensitized triplet chain cis-to-trans isomerizations of monoolefins in favorable situations.[4−8] In addition, quantum yields for cis/trans isomerizations of dienes of ~20 have been reported at low conversions.[9−11] Quantum chain reactions involving cis/trans isomerization are not likely to result in large refractive index changes, however.

Valence isomerizations can lead to large changes in the refractive index due to changes in conjugation. A modest quantum yield (~3) has been reported for the triplet chain isomerization of benzvalene to benzene.[2] The triplet-state chain isomerization of Dewar benzene has also been reported.[3] Unfortunately, the experimentally measured quantum yield for the latter reaction is quite low (~0.5), although a quantum yield as high as ~10 has been inferred by extrapolation.

Herein we report highly efficient triplet-sensitized quantum chain isomerizations of several substituted Dewar benzene derivatives. Quantum yields of >100 have been measured, and importantly, considerable chain amplification is maintained even at high reactant-to-product conversions. In addition, we have determined the energetic and complete kinetic factors that facilitate the high chain efficiencies. This study focuses on the triplet-sensitized photoisomerizations *in solution* and provides a detailed understanding of the fundamental processes. A future paper will address the same isomerizations in polymeric media, which have led to new information storage materials with improved photosensitivities and potentially high information densities.[12]

It is helpful to briefly consider the general energetic and kinetic factors that facilitate efficient triplet chain isomerization reactions. An energy level diagram of reactant (R) and product

* To whom correspondence should be addressed. E-mail: pmerkel@rochester.rr.com (P.B.M.); jpd@chem.rochester.edu (J.P.D.); farid@chem.rochester.edu (S.F.).
† University of Rochester.
‡ Eastman Kodak Co.

10.1021/jp067485j CCC: $37.00
Published on Web 02/01/2007

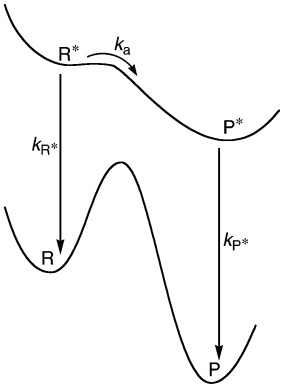

Figure 1. Energy level scheme for facile chain photoconversion of reactant (R) to product (P) via an electronically (usually triplet) excited state.

(P) ground and excited states similar to that in Figure 1 can result in high quantum yields that are maintained even at high levels of conversion. The excited state of the reactant (R*) is commonly produced by energy transfer from a photoexcited sensitizer with higher excitation energy. The salient features necessary for efficient photoisomerization include (a) adiabatic[13] conversion of R* to an excited product (P*) with little or no activation barrier, which results in a relatively large adiabatic isomerization rate constant, k_a, (b) an absolute R* energy that is above that of P*, (c) a larger excitation energy for P than R, i.e., $(E_{P*} - E_P) > (E_{R*} - E_R)$, which promotes chain propagation via exothermic energy transfer from P* to R in diffusional encounters, and (d) relatively small values of the decay constants for R* and P*, k_{R*} and k_{P*}, respectively, which minimize chain termination processes.[14] As will be shown, the Dewar benzene derivatives described in this study possess all of these optimal features.

Results and Discussion

Three Dewar benzene derivatives were used in this study, DB1−DB3. These derivatives were selected largely on the basis of ease of synthesis and also because of their reasonable thermal stability. The most extensive measurements were performed on the monoester, DB2, and the diester, DB3. We begin with a detailed discussion of the energetics for the quantum chain isomerizations, which is followed by the kinetics and quantum yield experiments.

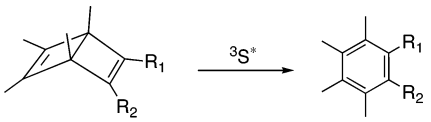

	R_1	R_2	
DB1	Me	Me	B1
DB2	CO_2Me	Me	B2
DB3	CO_2Me	CO_2Me	B3

1. Energetics. An examination of the excited-state energetics was useful to confirm that the photosensitized isomerizations of DB1−DB3 described in this work do *not* proceed by an electron-transfer chain mechanism.[15,16] Consider, for example, the photoinduced isomerization of DB1 with 2,4-diethylthioxanthone (DETX) as the sensitizer in ethyl acetate. DETX has a triplet energy of 63.5 kcal/mol (2.75 eV, vide infra) and a reduction potential of −1.62 vs SCE.[17] The oxidation potential of DB1 is ∼1.6 V vs SCE.[16] Thus, electron transfer from DB1 to DETX* would be endothermic by ∼0.5 eV. Importantly, DB3 is expected to be significantly harder to oxidize than DB1, yet the rate constant for quenching of triplet DETX by DB3 is over 100 times *greater* than that for quenching of triplet DETX by DB1. In addition, as shown below, the quenching rate constants of the triplet sensitizers are a smooth function of the triplet energies, regardless of variations in their reduction potentials. Furthermore, propagation of electron-transfer chain reactions is largely limited to polar solvents, which allows for separation of the radical ion pairs. In less polar solvents, however, the quantum yields are reduced to near unity. Finally, no product radical cations (absorption in the 460−490 nm range) were observed in flash photolysis experiments when triplet DETX was quenched by the Dewar benzenes of this study in ethyl acetate or in acetonitrile.

To better understand the energetics of the triplet chain isomerization process and to select optimal sensitizers to initiate the isomerization of the Dewar benzene derivatives, it is useful to evaluate their triplet energies. The most common method for determining triplet energies is from low-temperature phosphorescence spectra. However, none of the Dewar benzenes of this study phosphoresce, even in the presence of heavy atom additives, such as *n*-butyl iodide. An alternative method for determining the triplet energy of an acceptor, in this case E_T^R, first applied by Sandros,[18] is from plots of the logarithm of the rate constant for energy-transfer quenching (k_q) of a series of triplet energy sensitizers (S) vs the sensitizer triplet energy (E_T^S). In the Sandros model, k_q is related to the change in free energy (ΔG) associated with the triplet-energy-transfer process according to eq 1, wherein k_d is the rate constant for diffusional encounter between S^* and R. ΔG is assumed to equal the difference between the triplet-state energies of R and S ($\Delta G = E_T^R - E_T^S$).

$$k_q = \frac{k_d}{1 + \exp\left(\frac{\Delta G}{RT}\right)} \quad (1)$$

According to eq 1, k_q will approach k_d for sufficiently exothermic energy transfer (ΔG more negative than ∼2 kcal/mol). However, quenching by acceptor molecules in which the triplet state is distorted relative to the ground state, i.e., in which the equilibrium nuclear geometry is substantially different in the triplet state, will generally not obey the Sandros expression.[19] Instead, the falloff in k_q with increasingly positive ΔG will be more gradual. One comprehensive model for treating triplet energy transfer that has been applied with some success is the activation model of Balzani and co-workers.[19,20] A key factor in this model is the activation energy ($\Delta G^{\ddagger}$) for energy transfer analogous to that for electron transfer, which may be related to the standard free activation energy ($\Delta G_0^{\ddagger}$). Another key feature is the preexponential factor for forward energy transfer (k_{en}^0), whose magnitude may be reduced due to poor overlap of electronic orbitals or to unfavorable Frank−Condon factors between the initial and final states, to the extent that they are not fully reflected in $\Delta G^{\ddagger}$. According to the activation model, the experimental energy-transfer rate constant, k_q, is given by eq 2, where k_{-d} is the rate constant for dissociation of the

$$k_q = \frac{k_d}{1 + \frac{k_{-d}}{k_{en}} + \exp\left(\frac{\Delta G}{RT}\right)} \quad (2)$$

encounter complex between S* and R and

$$k_{en} = k_{en}^0 \exp\left(-\frac{\Delta G^{\ddagger}}{RT}\right)$$

$$\Delta G^{\ddagger} = \Delta G + \left(\frac{\Delta G_0^{\ddagger}}{\ln 2}\right) \ln\left\{1 + \exp\left(-\frac{\Delta G \ln 2}{\Delta G_0^{\ddagger}}\right)\right\}$$

In our analyses of energy transfer to Dewar benzenes we have used thermodynamic sensitizer triplet energies recently measured[21] by a flash photolysis technique.[22] These energies are preferable to triplet energies taken from low-temperature phosphorescence data, which may apply to a different solvent and lack possible entropy contributions to ΔG.[23] The thermodynamic procedure cannot be applied to the Dewar benzenes because their triplet lifetimes are far too short (see below). Instead the activation model was used. Plots of log k_q vs E_T^S for DB2 and DB3 in ethyl acetate[24] are given in Figure 2 (for details see the Supporting Information). The solid lines represent best fits of the experimental data according to eq 2. For this fitting, k_d was taken as 1.3×10^{10} M^{-1} s^{-1} on the basis of the solvent viscosity[25] and the ratio k_{-d}/k_{en}^0 was estimated to be 1.2 on the basis of asymptotic k_q values at high exothermicities. For the monoester reactant, DB2, the best fit is obtained with $E_T^R = 60 \pm 1$ kcal/mol and $\Delta G_0^{\ddagger} = 3.5 \pm 0.5$ kcal/mol, and for the diester reactant, DB3, with $E_T^R = 52.5 \pm 1$ kcal/mol and $\Delta G_0^{\ddagger} = 4 \pm 0.5$ kcal/mol. These fitting curves are contrasted with those that would be expected for the same E_T^R but with $\Delta G_0^{\ddagger} \approx 0$, i.e., having a slope corresponding to that of classical Sandros-type behavior (dashed curves in Figure 2).

Similarly, from a limited number of data points for DB1, the best fit energy-transfer parameters are $E_T^R = 64.5 \pm 1.5$ kcal/mol and $\Delta G_0^{\ddagger} = 3 \pm 1$ kcal/mol. The $\Delta G_0^{\ddagger}$ values of about 3−4 kcal/mol are similar to that of *cis*-stilbene[19] and not unreasonable for a triplet state that may have reduced double bond character. The decrease in triplet energies from DB1 to DB3 can be attributed to extended conjugation upon carboxylate substitution, as seen for other olefins.[26]

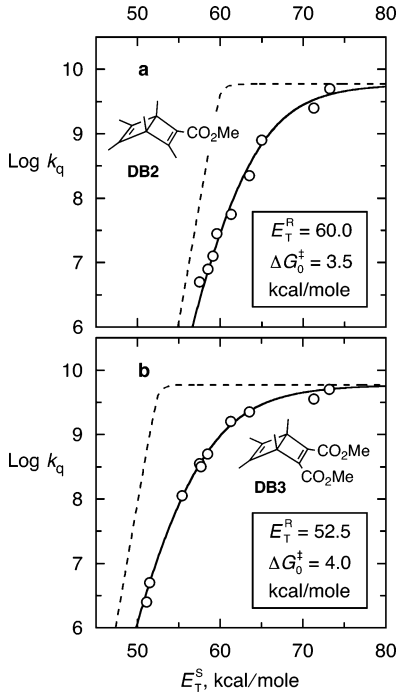

Figure 2. Rate constants for energy transfer from triplet donors to Dewar benzene reactants, DB2 (a; the corresponding ethyl ester was used in most of these measurements) and DB3 (b), vs thermodynamic triplet energies of the sensitizers (E_T^S) in ethyl acetate (see the Supporting Information). The solid curves were calculated according to eq 2 with $k_d = 1.3 \times 10^{10}$ s^{-1} and $k_{-d}/k_{en}^0 = 1.2$ and with the reactant triplet energies and activation parameters $\Delta G_0^{\ddagger}$ (see the text) given in the figure. The dashed curves are the values calculated for the same triplet energies but with $\Delta G_0^{\ddagger} \approx 0$.

Whereas the quenching data for the reactants DB2 and DB3 in Figure 2 appear to be well fit by this model, the E_T^R values thereby obtained may not represent true minima in the triplet potential energy surfaces.[27] Figure 2 clearly illustrates the nonclassical nature of the transfer of triplet energy to the Dewar benzenes, however.

An alternative quantitative analysis of nonclassical or "non-vertical" triplet energy transfer has recently been offered.[28] This analysis explicitly models the thermal ("hot-band") population of molecular configurations (typically involving torsional motions) of the acceptor ground state that provide lower energy vertical pathways to the excited triplet. In its most general form, the hot-band model does not require that the fully relaxed configuration of the acceptor triplet be thermally accessible or even that a minimum exists in the triplet potential energy surface. This situation may well apply to the Dewar benzenes of this study.

Although knowledge of the exact triplet energies of the benzene products is not critical to understanding the Dewar benzene isomerization kinetics and efficiencies, it was useful to determine the expected high E_T values of these adiabatically formed products to confirm that chain propagation energy transfer from the benzene triplets to the Dewar benzenes is energetically favorable. The phosphorescence of dilute solutions of the substituted benzene products was measured at 77 K in both hexane and ethyl acetate. Energies and spectral envelopes were similar in both solvents with poor to fair resolution of the 0−0 vibronic band. Hexane generally provided a somewhat better definition of the 0−0 band. E_T values for the benzene products, B1−B3, were all approximately 74 kcal/mol.

An attempt was also made to measure thermodynamic E_T values of the benzene products from equilibration experiments[22] using xanthone and thioxanthone derivatives as sensitizers. The thermodynamic triplet energies were found to be lower than those determined from phosphorescence spectra. For example, the thermodynamic E_T value for B3 obtained from equilibration with triplet 3-methoxythioxanthone ($E_T = 67.0$ kcal/mol[21]) was 68.5 ± 0.5 kcal/mol, ~5.5 kcal/mol lower than the triplet energy determined from phosphorescence. The thermodynamic E_T for B2 was similarly determined to be ~69 kcal/mol.[29] Strong photoproduct absorption, perhaps due to radical species, precluded accurate measurement of a thermodynamic E_T for B1. The smaller thermodynamic triplet energies determined for B2 and B3 contrasts with those obtained for *unstrained* benzene derivatives, such as dimethyl terephthalate, which shows nearly identical phosphorescence and thermodynamic E_T values of 73.0 and 72.8 kcal/mol, respectively.[21] Perhaps the phosphorescence from the highly substituted benzenes (B1−B3) at low temperature occurs largely from molecules frozen in slightly higher energy conformations.[30]

An energy level diagram for the DB3/B3 system based on the triplet energy measurements is shown in Figure 3. The energy of the DB3 ground state relative to B3 was estimated to be ~59 kcal/mol on the basis of the effects of methyl and ester substituents on the energies of Dewar benzene derivatives determined from ab initio calculations.[31] Clearly, the energy content of DB3* is more than sufficient to produce B3* from adiabatic isomerization. In addition, the energy of B3* is high

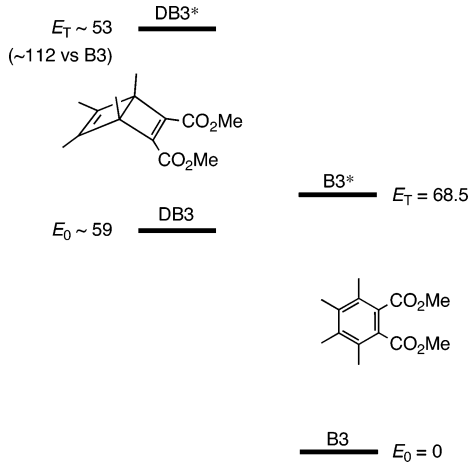

Figure 3. Energy levels (kcal/mol) for the DB3/B3 system.

SCHEME 1

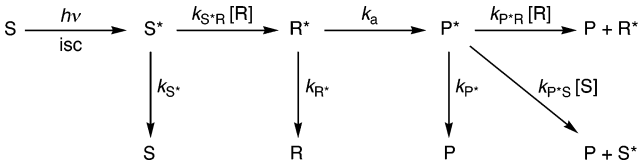

enough for efficient transfer to DB3 for chain propagation. Similar situations obtain for the DB1/B1 and DB2/B2 pairs.

2. Kinetic Scheme. The pertinent reactions required to explain all transient and steady-state kinetic data for triplet chain isomerization of the Dewar benzene reactants, R, to corresponding benzene products, P, are outlined in Scheme 1, where S is a triplet sensitizer. For the systems described here, all processes are essentially irreversible.

The bimolecular rate constants k_{S^*R}, k_{P^*R}, and k_{P^*S} are for energy transfer from the triplet sensitizer (S*) to the reactant (R), the triplet product (P*) to the reactant, and the triplet product to the sensitizer, respectively; k_a is the unimolecular rate constant for the adiabatic isomerization of R* to P*. The rate constants k_{S^*} and k_{P^*} represent the sum of all decays of these triplet species (eqs 3 and 4,

$$k_{S^*} = k'_{S^*} + k_{S^*i(R)}[R] + k_{S^*i(S)}[S] + k_{S^*Q}[Q] \qquad (3)$$

$$k_{P^*} = k'_{P^*} + k_{P^*i(R)}[R] + k_{P^*i(S)}[S] + k_{P^*Q}[Q] \qquad (4)$$

where k'_{S^*} is the decay rate constant of the excited sensitizer, $k_{S^*i(R)}$ and $k_{S^*i(S)}$ are quenching rate constants of the triplet sensitizer by trace impurities in R or S multiplied by the molar fraction of these impurities, and k_{S^*Q} is the rate constant for quenching of S* by a quencher (Q), added at specific concentrations to allow the determination of some of the other rate constants). Analogously, k_{P^*} represents the corresponding reactions of P*. As will be shown later, the decay rate constant of R*, k_{R^*}, is negligibly small compared to the adiabatic isomerization rate constant, k_a. On the basis of Scheme 1 and given that $k_{R^*} \ll k_a$, the isomerization quantum yield (Φ_{isom}) is given by eq 5 (see the Supporting Information), where Φ_{isc} is the

$$\Phi_{isom} = \Phi_{isc}\alpha\frac{k_{P^*} + k_{P^*S}[S] + k_{P^*R}[R]}{k_{P^*} + (1-\alpha)k_{P^*S}[S]} \qquad (5)$$

intersystem crossing quantum yield of the sensitizer and α is the fraction of S* that leads to the formation of R*:

$$\alpha = \frac{k_{S^*R}[R]}{k_{S^*R}[R] + k_{S^*}}$$

3. Transient Kinetics. A combination of transient and steady-state measurements was necessary to fully elucidate the kinetics of the chain-amplified isomerization. This section deals with the transient (laser flash photolysis) experiments and is subdivided into three parts to determine rate constants for (1) energy-transfer reactions, (2) deactivation by added quencher, and (3) cage kinetics and adiabatic isomerization. In the course of these investigations, three different sensitizers were used: 2,4-diethylthioxanthone (DETX), 2-*tert*-pentylxanthone (PXN), and 1-methylphenanthrene (1MP). Methyl 1-pyrenebutyrate (MPB) was used as a triplet-state quencher.

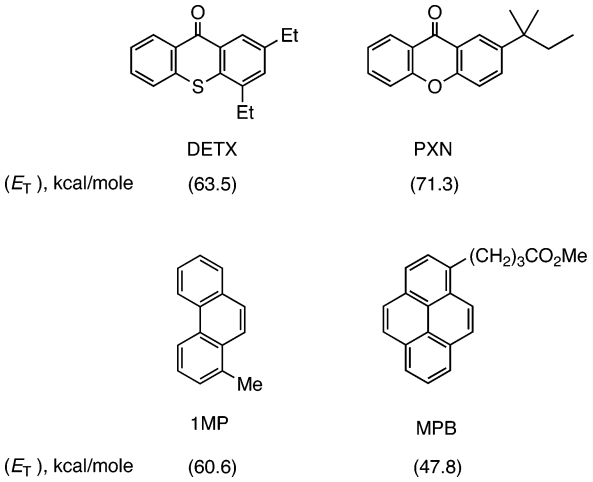

3.1. Energy-Transfer Rate Constants. It is desirable to use a sensitizer with considerably higher triplet energy than that of the reactant to maximize the forward energy transfer (k_{S^*R}, Scheme 1) and minimize reverse energy transfer. However, even with a high-energy sensitizer, energy transfer from the higher energy triplet product (P*) (produced by adiabatic isomerization of R*) to S (k_{P^*S}) will take place. The following experiments were designed to determine two of the energy-transfer rate constants given in Scheme 1, k_{S^*R} and k_{P^*S}. The third, k_{P^*R}, could be obtained only from steady-state experiments (see below).

Using DETX as the sensitizer (S), the decay of the triplet (S*) at 650 nm ($\epsilon \approx 30000$) was monitored at different concentrations of the reactant DB2 as shown in Figure 4. The initial rapid decay of S* (the only species absorbing at 650 nm), which increases with increasing reactant concentration, corresponds largely to the energy transfer quenching of S* by R (k_{S^*R}, Scheme 1). Because S* is re-formed through energy transfer from P* to S (k_{P^*S}), a quasi-equilibrium between S* and P* is established, reflected by the slower component in the biexponential decay of S* in Figure 4. As discussed below, the adiabatic isomerization (k_a, Scheme 1) is very fast compared to the other reactions in the scheme, and as a result, negligible R* exists in quasi-equilibrium with S* and P*. Analysis of the transient kinetics of S* can, therefore, be simplified to eq 6,

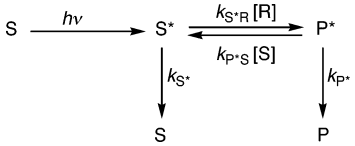

(6)

and the decay of S* analyzed using the well-known solution given by eq 7a, where the two decay constants λ_1 and λ_2 and

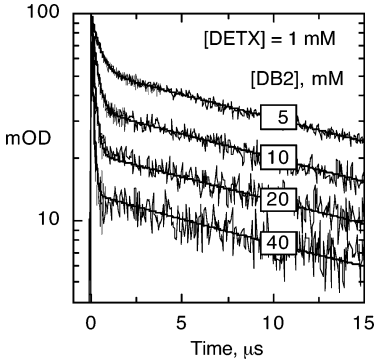

Figure 4. Decay of the triplet sensitizer (DETX*), monitored at 650 nm, following pulsed excitation (7 ns, at 343 nm) of an Ar-purged ethyl acetate solution of DETX (1 mM) and the reactant DB2 at the millimolar concentrations given in the figure. The measurements were carried out on two time scales for higher accuracy of the fitting of the fast and slow decays. The fittings (smooth curves) were carried out globally on both sets of data.

the ratio of the preexponentials A_1/A_2 are given by eqs 7b−d,[32,33]

$$\mathrm{OD} = A_1 \exp(-\lambda_1 t) + A_2 \exp(-\lambda_2 t) \tag{7a}$$

$$\lambda_1 = 0.5(X + Y) + 0.5\{(X - Y)^2 + 4k_{S*R}[R]k_{P*S}[S]\}^{1/2} \tag{7b}$$

$$\lambda_2 = 0.5(X + Y) - 0.5\{(X - Y)^2 + 4k_{S*R}[R]k_{P*S}[S]\}^{1/2} \tag{7c}$$

$$A_1/A_2 = (X - \lambda_2)/(\lambda_1 - X) \tag{7d}$$

$$X = k_{S*} + k_{S*R}[R]$$

$$Y = k_{P*} + k_{P*S}[S]$$

As expected, the ratio A_1/A_2 in Figure 4 increases with increasing [R]/[S] ratio. From these ratios and the decay constants, values for k_{S*R} of 2.1×10^8 M^{-1} s^{-1} and for k_{P*S} of 1.2×10^9 M^{-1} s^{-1} were reliably determined.

To test the proposed kinetic scheme in eq 6, we sought an independent determination of k_{P*S} to confirm the rather indirectly obtained value mentioned above. This was achieved through generation of the triplet benzene product (P*) by energy transfer from another, higher energy triplet sensitizer *directly* to the benzene product, B2 in this case. An ethyl acetate solution of PXN (E_T = 71.3 kcal/mol[21]), 0.12 M B2, and 0.5 mM DETX was excited with 343 nm laser pulses. PXN absorbs most of the laser light to form PXN*, which is rapidly quenched (spike close to $t = 0$ in Figure 5) primarily by B2 (due to its high concentration) to yield B2* (PXN* + B2 → PXN + B2*). The buildup of DETX* by quenching of B2* (B2* + DETX → B2 + DETX*) was followed at 650 nm. Fitting of the experimental data (Figure 5) gave a value for k_{P*S} of $(\sim 1.2 \pm 0.1) \times 10^9$ M^{-1} s^{-1}, which is the same as that obtained from the experiment mentioned above, lending further support to the kinetic scheme.

3.2. Quenching Rate Constants. To fully elucidate the mechanism outlined in Scheme 1, it was necessary to carry out measurements of isomerization quantum yields in the presence of an added quencher, Q (see the steady-state experiments below). MPB proved to be well suited because of its low triplet energy and its resistance to photodegradation.

The quenching of S* by Q was obtained in a straightforward experiment from the pseudo-first-order decay of S* as a function

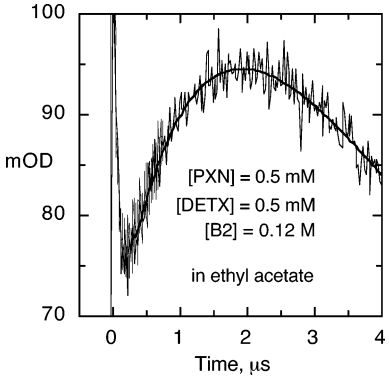

Figure 5. Growth and decay of DETX*, monitored at 650 nm, following pulsed excitation (343 nm) of a solution of PXN, DETX, and the benzene product B2 (see the text for details). The measurements were carried out on two time scales (0.8 and 8 μs with only a portion of the latter shown) for higher accuracy of the fitting. The fitting (smooth curve) was carried out globally on both sets of data.

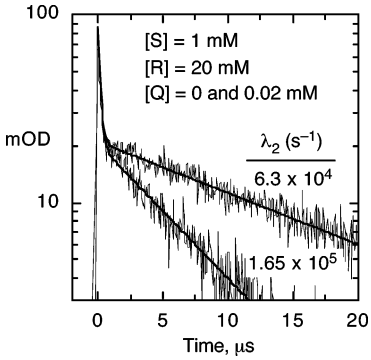

Figure 6. Decay of the triplet sensitizer (DETX*), monitored at 650 nm, following pulsed excitation (7 ns, at 343 nm) of an Ar-purged ethyl acetate solution of DETX (1 mM) and the reactant DB2 (20 mM) in the presence and absence of a quencher (MPB).

of [Q], which gave a value of 6.5×10^9 M^{-1} s^{-1} for the rate constant, k_{S*Q}, eq 1. The quenching rate constant of P* by Q, k_{P*Q}, was determined from fittings of the double-exponential decays (similar to those shown in Figure 4) in the presence of varied concentrations of Q. Due to the high triplet energy of P*, it was more convenient to generate P* by reaction of S* with R, which, as mentioned above, results in a much larger quasi-equilibrium concentration of P* than R*. As shown in Figure 6, the kinetic parameter most affected by the added quencher is λ_2 (cf. eq 7). From kinetic fitting, k_{P*Q} was determined to be 4×10^9 M^{-1} s^{-1} for DB2.

3.3. Encounter Complex/Cage Kinetics. In principle, the isomerization of triplet reactant to triplet product, R* → P*, can be followed by the T−T absorption of P* in the region of about 310−340 nm. When a high-energy sensitizer is used, rapid energy transfer from S* to R occurs, and the subsequent formation of P* can be probed. A deoxygenated solution of 0.1 mM PXN plus 0.1 M DB2 in ethyl acetate was excited with 7 ns, 343 nm laser pulses. At this [DB2], the initially formed PXN* is fully quenched within ~10 ns. The formation of B2* monitored at 325 and 340 nm occurs within the same time frame, with *no* apparent time lag. This implies that adiabatic isomerization of DB2 occurs with $k_a \geq 2 \times 10^8$ s^{-1} in ethyl acetate, thereby establishing a *lower limit* for k_a.

If k_a is large enough to compete with the rate constant for dissociation of the encounter complex between R* and S, then the kinetic scheme must explicitly include *isomerization within the encounter complex* (i.e., cage isomerization). For this situation, the relevant kinetic processes are shown in Scheme

SCHEME 2

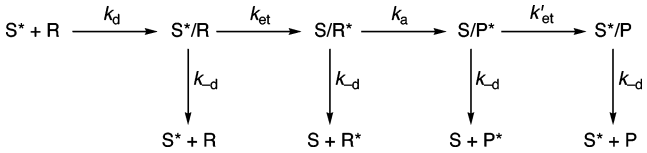

2, where k_d is the diffusional rate constant for formation of an encounter complex, k_{-d} is the encounter complex separation rate constant, k_a is the rate constant for adiabatic isomerization, and the rate constants for energy transfer *within* the encounter complexes are k_{et} and k'_{et}.

In cases where reverse energy transfer from R* to S can be ruled out on an energetic basis, the experimentally measured rate constant for quenching of S* with R (k_{S*R}) in Scheme 2 is given by eq 8.

$$k_{S*R} = k_d\beta(1 - \gamma\delta) \tag{8}$$

$$\beta = \frac{k_{et}}{k_{et} + k_{-d}} \qquad \gamma = \frac{k_a}{k_a + k_{-d}} \qquad \delta = \frac{k'_{et}}{k'_{et} + k_{-d}}$$

Scheme 2 has a total of 5 mechanistic rate constants. As we will show, k_d and k_{-d} can be determined by standard means. The rate constant for in-cage energy transfer from P* to S, k'_{et}, can be determined from measurements of k_{P*S} as previously described in section 3.1. The two remaining rate constants, k_a and k_{et}, can be determined by measuring k_{S*R} in two solvents of differing viscosity. According to eq 8, if a low-viscosity solvent is used such that $k_a \ll k_{-d}$, and/or $k'_{et} \ll k_{-d}$, the measured rate constants k_{S*R} will approach $k_d\beta$, the predicted rate constant in the absence of in-cage isomerization and of subsequent energy transfer to re-form S*. When a solvent of higher viscosity is used, however, k_{-d} will decrease and the terms γ and δ in eq 8 will increase. As the contributions from these terms increase, the measured k_{S*R} decreases relative to $k_d\beta$; i.e., the *effective* quenching decreases due to re-formation of S* within the cage. Thus, the change in k_{S*R} as a function of solvent viscosity provides a kinetic strategy for determining k_a. To obtain a value for k_a with reasonable accuracy, however, it is necessary that one of the solvents has a k_{-d} in the range of k_a and k'_{et} to increase the deviation of k_{S*R} from $k_d\beta$ and thus allow both k_a and k_{et} to be determined. It turned out that bis-(2-ethylhexyl) adipate (usually referred to as dioctyl adipate, DOA), which was used as a more viscous ($\eta \approx 16$ cP) analogue of ethyl acetate ($\eta \approx 0.5$ cP), worked well in this regard.

3.3.1. Diffusion-Dependent Rate Constants k_d and k_{-d}. The diffusion rate constant for encounter, k_d, in ethyl acetate was taken to be 1.3×10^{10} M^{-1} s^{-1},[25] and the corresponding dissociation rate constant, k_{-d}, was calculated from Eigen's expression[34] as 3.0×10^{10} s^{-1}. Values for k_d and k_{-d} in DOA were determined by comparison of energy-transfer rates in ethyl acetate and DOA. The nearly diffusion-limited energy-transfer rate from DETX* to 1,4-dibromonaphthalene (DBN, thermodynamic $E_T = 57.5$ kcal/mol[21]) aided in this determination. Because this energy transfer is quite exothermic, reverse energy transfer (eq 2) from DBN* to DETX can be ruled out, and the measured quenching rate constant k_q is given by eq 9.

$$k_q = k_d \frac{k_{et}}{k_{et} + k_{-d}} \tag{9}$$

From the measured quenching rate constant (k_q) of 7.6×10^9 M^{-1} s^{-1} for DETX* by DBN in ethyl acetate and the above-noted values k_d and k_{-d} in ethyl acetate, an in-cage energy-transfer rate constant (k_{et}) of 4.2×10^{10} s^{-1} is obtained. The value of k_{et} is expected to be independent of the solvent viscosity and therefore also applies in DOA. For quenching of DETX* by DBN in DOA a quenching rate constant (k_q) of 8.5×10^8 M^{-1} s^{-1} was measured. Substituting this value and that for k_{et} into eq 9, and using the same ratio of k_{-d}/k_d as that for ethyl acetate,[35] yields values for $k_d = 8.9 \times 10^8$ M^{-1} s^{-1} and $k_{-d} = 2.05 \times 10^9$ s^{-1} in DOA. It is worth noting that because of the small value of k_{-d} in DOA, the measured k_q for a considerably exothermic energy-transfer reaction is nearly equal to k_d. The value of k_d in DOA determined in this way is likely, therefore, to be quite accurate.

3.3.2. Selection of Appropriate Sensitizers. For accurate determination of k_a it is important to choose a sensitizer that meets two conditions. First, the ultimate accuracy of k_a will increase with increasing contribution from re-formed S* in Scheme 2, i.e., with increasing k'_{et}. The use of a low-energy triplet sensitizer increases the exothermicity of energy transfer from P* to S and consequently k'_{et}. Second, and more importantly, determination of the adiabatic rate constant as outlined above is based on measurements in two different solvents, with the assumption that both in-cage energy-transfer rate constants, k_{et} and k'_{et}, remain solvent independent. It is, therefore, essential that the triplet energy of the sensitizer does not vary significantly with the solvent. Because of modest differences in polarity and polarizability between ethyl acetate and DOA, triplet energies of polar molecules such as DETX can vary slightly between the two media and complicate the analysis.[36] In contrast, triplet energies of simple aromatic hydrocarbons should be fairly insensitive to slight differences in solvent polarity and polarizability. 1MP ($E_T = 60.6$ kcal/mol[21]) proved to be a well-suited sensitizer for these experiments. Phosphorescence measurements at 77 K indicated that the triplet energy of 1MP is very insensitive to the solvent polarity and polarizability. This was further substantiated by measurement of the rate constants for energy-transfer quenching, k_q, from triplet 1MP* to tetrachloroethylene, TCE,[37] in ethyl acetate and in DOA. The experimental k_q value in ethyl acetate is 2.43×10^7 M^{-1} s^{-1}. This rate constant can be used to predict a value for k_q in DOA via eq 9. Gratifyingly, the predicted value of 2.37×10^7 M^{-1} s^{-1} in DOA exactly equals the experimental value, affirming that the in-cage energy-transfer rate constant, k_{et}, and consequently E_T of 1MP are essentially unchanged in ethyl acetate and DOA. The fact that the k_q values are so similar in ethyl acetate and DOA despite substantial differences in viscosity is fully anticipated from eq 9 when k_{et} is small and the k_{-d}/k_d ratio remains constant. Indeed, the similarity of the k_q values in ethyl acetate and DOA reinforces the applicability of the encounter complex model. (See the Supporting Information for comparative quenching plots in ethyl acetate vs DOA.)

3.3.3. In-Cage Energy-Transfer Rate Constant, k'_{et}. The bimolecular rate constants k_{P*S} and k_{S*R} in ethyl acetate and DOA were determined using 1MP as the sensitizer (0.5 mM) and DB2 as the reactant (0.1 M) by laser flash photolysis experiments analogous to those described above in section 3.1. As shown in Figure 7, the decay of 1MP* was fitted to two exponential decays according to eq 7, from which the decay constants, λ_1 and λ_2, and the ratio of their preexponentials, A_1/A_2, were obtained. Using these three kinetic parameters, and assuming $k_{S*} \approx k_{P*}$, values for the rate constants k_{S*R} and k_{P*S} were obtained (see Table 1). Because k_{S*} and k_{P*} are small compared to k_{S*R} and k_{P*S}, uncertainty in their absolute or relative values has a negligible effect on the latter rate constants.

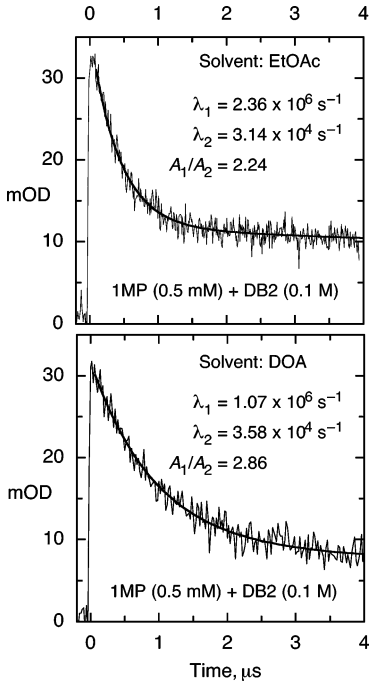

Figure 7. Decay of triplet 1-methylphenanthrene (1MP*) monitored at 492 nm, following 343 nm excitation of 1MP in the presence of DB2 in ethyl acetate (top) and in DOA (bottom). The experiments were also carried out on the 40 μs time scale (not shown) and the data analyzed globally, giving the parameters shown in the figure.

TABLE 1: Data from Laser Flash Photolysis of 1MP and DB2 in Ethyl Acetate and in DOA, Figure 7[a]

	EtOAc	DOA	units
λ_1	2.36×10^6	1.07×10^6	s^{-1}
λ_2	3.14×10^4	3.58×10^4	s^{-1}
A_1/A_2	2.24	2.86	
k_{S*R}	1.63×10^7	7.84×10^6	$M^{-1}\ s^{-1}$
k_{P*S}	1.47×10^9	5.70×10^8	$M^{-1}\ s^{-1}$
k_d	1.3×10^{10}	8.9×10^8	$M^{-1}\ s^{-1}$
k_{-d}	3.0×10^{10}	2.05×10^9	s^{-1}
k_{et}	3.8×10^9	3.7×10^9	s^{-1}

[a] The parameters λ_1, λ_2, and A_1/A_2 are obtained from data analysis according to eq 7, from which the rate constants k_{S*R} and k_{P*S} are calculated. The other rate constants are defined in Scheme 2 and determined as described in the text.

With values for k_{P*S}, k_d, and k_{-d} in hand, the rate constant for in-cage energy transfer from P* to S, k'_{et}, could be determined by using eq 10. Confidence in the applicability of

$$k_{P*S} = k_d \frac{k'_{et}}{k'_{et} + k_{-d}} \qquad (10)$$

the proposed cage model and the assumption of the solvent independence of the ratio k_{-d}/k_d was further strengthened by the fact that the value for k'_{et} obtained from the ethyl acetate experiment was very similar to that in DOA, 3.8×10^9 vs 3.7×10^9 s^{-1} (Table 1).

3.3.4. Adiabatic Rate Constant, k_a. The adiabatic isomerization rate constant, k_a, and the other in-cage energy-transfer rate constant, k_{et}, can be obtained from the experimental rate constants k_{S*R} in ethyl acetate and DOA. As shown in Table 1, the energy-transfer rate constant k_{S*R} for 1MP*/DB2 in DOA is distinctly lower than that in ethyl acetate, 7.84×10^6 vs 1.63×10^7 M^{-1} s^{-1}. This is in sharp contrast to the similarly slow reaction of 1MP* with TCE, which shows nearly identical quenching rate constants in both solvents (see above). On the basis of eq 9, the quenching rate constants by TCE are expected to be similar in both solvents because $k_{et} \ll k_{-d}$. Were it not for in-cage isomerization, the same behavior would be expected for the quenching of 1MP* by DB2. However, quenching by the Dewar benzene derivative leads to a greater amount of triplet sensitizer re-formed in DOA than ethyl acetate by in-cage return energy transfer from P*, which results in a lower net quenching rate constant in DOA than in ethyl acetate.

Substituting the experimental values of k_{S*R}, the values of k_d and k_{-d}, and an average value for k'_{et} of 3.75×10^9 s^{-1} (Table 1) into eq 8 and solving the two equations (ethyl acetate and DOA data) for the two unknowns, k_a and k_{et}, yielded 8.8×10^9 and 3.9×10^7 s^{-1}, respectively, for these rate constants. Some uncertainty in these rate constants derives from errors in the critical, experimental k_{S*R} and k_{P*S} values and uncertainty in the exact ratio of k_{-d}/k_d. The errors in k_{S*R} and k_{P*S} are estimated to be 10%. Combining these with a 20% variation in the ratio for k_{-d}/k_d of 2.3 leads to a k_a of $(9 \pm 5) \times 10^9$ s^{-1}. Although the adiabatic isomerization rate constant determined here strictly applies to an in-cage reaction, it seems reasonable to assume that the rate constant for the corresponding out-of-cage R* → P* reaction would be quite similar.

On the basis of the rate constants derived from Scheme 2, it is straightforward to show that the re-formation of S* through in-cage isomerization followed by in-cage back energy transfer from P* to S ($\gamma\delta$ in Scheme 2) is only ~2−3% in ethyl acetate but ~50% in the more viscous DOA. The very small effect of the in-cage reaction in ethyl acetate (which will be even smaller with DETX as the sensitizer due to a smaller k'_{et}) shows that the cage processes in Scheme 2 can be safely neglected for ethyl acetate. Consequently, the kinetic hypothesis illustrated in Scheme 1 can be used for the chain isomerization reactions in ethyl acetate.

The adiabatic isomerization rate constant, k_a, of the diester reactant DB3 was similarly determined from the rate constants k_{S*R} for 1MP*/DB3 in ethyl acetate (3×10^9 M^{-1} s^{-1}) and in DOA (4.2×10^8 M^{-1} s^{-1}) as described above for 1MP*/DB2. Because the contribution from re-formed S* is small in this case, k_{P*S} was obtained from a separate experiment analogous to that shown in Figure 5 rather than from data like those in Figure 4. In this experiment, triplet excited PXN transfers energy predominantly to B3 (present at relatively high concentration), which then transfers energy to 1MP. The rate constant of the latter reaction is derived from the growth rate of 1MP*. This experiment gives k_{P*S} for B3*/1MP of ~1.4×10^9 M^{-1} s^{-1} in ethyl acetate. From this and the rate constants k_{S*R} in the two solvents, k_a for DB3* → B3* was estimated to be ~4×10^9 s^{-1}.

4. Steady-State Kinetics and Isomerization Quantum Yields. The isomerization quantum yields (Φ_{isom}) were measured as a function of reactant, sensitizer, and quencher concentrations. Most isomerization quantum yields were measured in argon-purged ethyl acetate solutions; a few measurements carried out in benzene gave results nearly identical to those obtained in ethyl acetate. The isomerization quantum yields for DB2 were the most extensively investigated and will be discussed first. DETX (Φ_{isc} in ethyl acetate = 0.98) was used as the sensitizer (405 nm excitation) and MPB as a quencher in these experiments. In general, the reported quantum yields are typically an average of at least three independent determinations.

Besides quantum yields greater than unity, an additional characteristic expected for a quantum chain photoreaction is an increase in quantum yield with increasing R concentration, which largely reflects the importance of chain propagation by

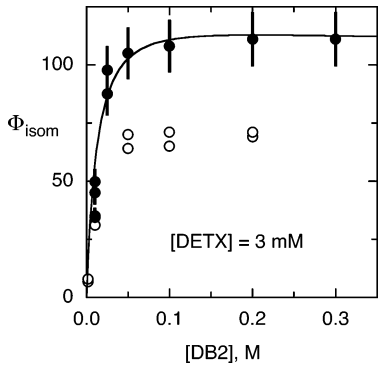

Figure 8. Dependence of the isomerization quantum yield on the reactant (DB2) concentration in argon-purged ethyl acetate, sensitized with DETX. After extensive purification (see the Experimental Section) of DB2, the data shown in open circles were obtained. Following another purification cycle, the data shown as closed circles were obtained. The curve was obtained from a global fitting (see the text) based on Scheme 1, eq 5, and the kinetic parameters in Table 2.

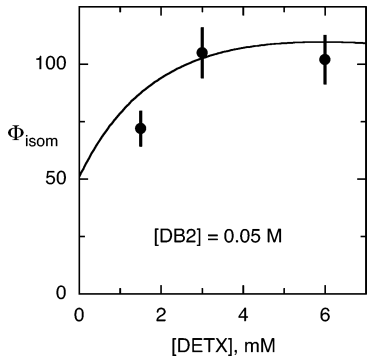

Figure 9. Dependence of the isomerization quantum yield of DB2 in argon-purged ethyl acetate on the sensitizer concentration, [DETX]. The curve was obtained from a global fitting (see the text) based on Scheme 1, eq 5, and the kinetic parameters in Table 2.

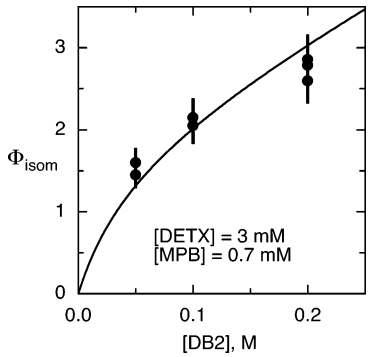

Figure 10. Dependence of the isomerization quantum yield on the reactant (DB2) concentration in argon-purged ethyl acetate, sensitized with DETX in the presence of 0.7 mM quencher (MPB). The curve was obtained from a global fitting (see the text) based on Scheme 1, eq 5, and the kinetic parameters in Table 2.

energy transfer from P* to R. In initial measurements, a plot of Φ_{isom} vs [DB2] showed a steep increase at reactant concentrations below ~0.05 M and a maximum of ~70 at [DB2] ≥ 0.05 M (open circles in Figure 8). It soon became apparent that the quantum yields were very sensitive to impurities in the Dewar benzene reactant (R) and the sensitizer (S). Thus, careful and repeated purifications were essential to maximize the quantum yields. For example, additional purification of DB2 by a cycle of column chromatography, recrystallization, and distillation led to a qualitatively similar dependence of Φ_{isom} on [DB2], but with a maximum quantum yield of ~110 (closed circles, Figure 8). Last, we note that the quantum yields at conversions of ~2% are slightly lower than those between ~2% and 10%, probably due to consumption of trace amounts of residual oxygen and/or some reactive impurity.

The quantum yield experiments illustrate both the chain nature of the process and the extreme sensitivity of the quantum yields to trace impurities in the reactant. The latter observation required the explicit inclusion of the impurity quenching processes in eqs 3 and 4 and Scheme 1. The quantum yield experiments also suggest that the limiting value of the quantum yield is due to competition between the propagation step, P* + R → P + R* (k_{P*R}, Scheme 1), and quenching of P* by impurities in the reactant ($k_{P*i(R)}$). The latter is the chain termination rate constant multiplied by the molar fraction of quenching impurities in the reactant. Since these two competing rates both increase linearly with [R], the quantum yield plateau is an approximate measure of the ratio $k_{P*R}/k_{P*i(R)}$.

The transient experiments (section 3.1) showed that the triplet product, P*, is intercepted by the sensitizer to regenerate another S* molecule, constituting an additional chain propagation process. The quantum yields, corrected for incomplete absorption by the sensitizer at lower concentrations, could therefore depend on [S]. Figure 9 shows an initial increase in Φ_{isom} followed by a leveling off at higher [S], analogous to the dependence of Φ_{isom} on [R]. This effect may also be attributed to residual impurities in the sensitizer, in spite of several purification steps.

Determination of the energy-transfer propagation rate constant, k_{P*R}, is made possible by establishing a competition between this step and a termination reaction that proceeds at a known rate. The rate constants for interception of both S* and P* by an added low-triplet-energy quencher, MPB, were determined by laser flash photolysis (see section 3.2). The effect of this quencher (Q) on the quantum yield was evaluated in two experiments: by varying [R] at constant [Q] (Figure 10) and by varying [Q] at constant [R] (Figure 11).

At low quencher concentrations, the change in Φ_{isom} (Figures 10 and 11a) is most sensitive to the ratio of propagation (k_{P*R}) to quenching (k_{P*Q}) rate constants. At high quencher concentration the chain propagation is practically eliminated, and the effect of quencher on the quantum yield is predominantly due to interception of S* (see Figure 11b).

The fitted lines shown in Figures 8−11 were derived from a global analysis of the combined data of *all* these quantum yield experiments according to Scheme 1 and eq 5. Some of the rate constants were obtained from transient kinetics (section 3), given in parentheses in Table 2, and were used as fixed parameters in the fitting procedure. Although less sensitive to the deactivation processes by impurities, the λ_1 and A_1/A_2 parameters of the transient data were also fitted using the same set of rate constants (Table 2) used for the quantum yield data (see the Supporting Information). However, the corresponding λ_2 values (the slow decay component) were higher than predicted by ~3×10^4 s^{-1}. This can be attributed to quenching by residual oxygen (~10^{-5} M) in the transient experiments. As mentioned above, the isomerization quantum yield did increase after a short exposure time, during which the residual oxygen was presumably consumed.

The rate constants in Table 2 were also used to fit the percent conversion as a function of irradiation time. The change in slope of such a plot corresponds to the change in quantum yield as the conversion increases. Shown in Figure 12 are the experimentally measured data points starting with [DB2] of 0.05 and of 0.1 M, together with the predicted curves. As the conversion

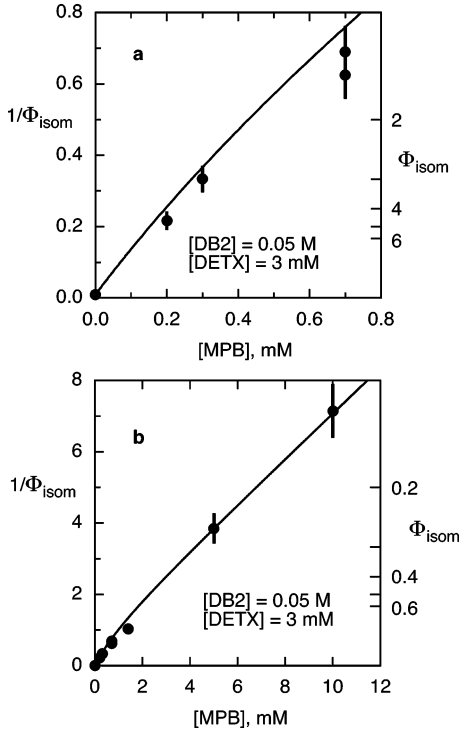

Figure 11. Dependence of the isomerization quantum yield of DB2 on the quencher (MPB) concentration (up to 0.8 mM (a) and to 12 mM (b)) in argon-purged ethyl acetate, sensitized with DETX. The curves were obtained from a global fitting (see the text) based on Scheme 1, eq 5, and the kinetic parameters in Table 2.

TABLE 2: Rate Constants of the Triplet Product (P*) and Triplet Sensitizer (S*) Involved in the Chain Isomerization of DB2 as the Reactant (R) and DEXT as the Sensitizer (S) in Ethyl Acetate[a]

reactions of P*		reactions of S*	
k_{P*R}	2.3×10^7 M^{-1} s^{-1}	k_{S*R}	$(2.1 \times 10^8$ M^{-1} $s^{-1})$
k_{P*S}	$(1.2 \times 10^9$ M^{-1} $s^{-1})$		
k_{P*Q}	$(4.0 \times 10^9$ M^{-1} $s^{-1})$	k_{S*Q}	$(6.5 \times 10^9$ M^{-1} $s^{-1})$
$k_{P*i(R)}$	2.1×10^5 M^{-1} s^{-1}	$k_{S*i(R)}$	4.0×10^5 M^{-1} s^{-1}
$k_{P*i(S)}$	3.0×10^6 M^{-1} s^{-1}	$k_{S*i(S)}$	3.0×10^6 M^{-1} s^{-1}
k_{P*}	1.2×10^4 s^{-1}	k_{S*}	1.2×10^4 s^{-1}

[a] MPB was used as the quencher (Q). The values in parentheses were obtained from transient experiments (section 3), the rest from fitting the quantum yield data (Figures 8−11) according to eq 5. The rate constants are defined in Scheme 1 and eqs 3 and 4.

increases the ratio of reactant to impurity decreases, leading to an accelerated decrease in quantum yield. The fit is very good up to ~70% conversion with slight deviation at higher conversion, possibly due to a minor side reaction yielding an additional quenching product.

The chain termination of the triplet sensitizer through quenching by impurities in the reactant ($k_{S*i(R)}$) and sensitizer ($k_{S*i(S)}$) and the corresponding deactivation of the triplet product (via $k_{P*i(R)}$ and $k_{P*i(S)}$) depend on the sample purity and are not "intrinsic" to the system. The critical rate constant for chain propagation, the energy transfer from triplet product to reactant (k_{P*R}), however, is intrinsic to the system. Although this energy transfer is exothermic, k_{P*R} for B2*/DB2 obtained from the global fitting is only 2.3×10^7 M^{-1} s^{-1}, more than 2 orders of magnitude less than the diffusion-controlled limit. This can be attributed to the differences in nuclear configurations between ground and triplet states of the Dewar benzene, *and* of the corresponding, sterically crowded benzene product (see section 1). The large nuclear changes that must accompany energetically

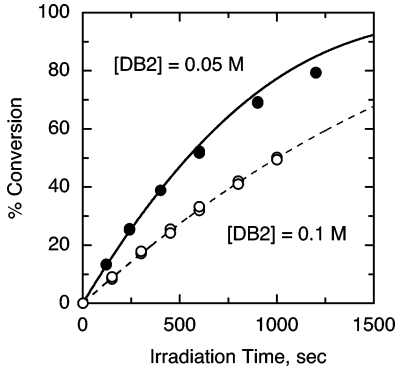

Figure 12. Percent conversion of DB2 to B2 in argon-purged ethyl acetate, sensitized with DETX, starting with [DB2] = 0.05 M (closed circles) and 0.1 M (open circles). The curves were obtained from a global fitting (see the text) based on Scheme 1, eq 5, and the kinetic parameters in Table 2.

favorable energy transfer when both the donor and acceptor possess distorted triplet states can severely restrict transfer rates, as was noted previously for a series of such triplet energy donors and acceptors.[38] It is the low value of k_{P*R} that makes Φ_{isom} very sensitive to impurities. If the impurities in the reactant and sensitizer were to be completely eliminated, the isomerization quantum yield of DB2 would continue to increase with the reactant concentration and at 0.5 M would exceed 1000!

Photolysis experiments similar to those of DB2 were also carried out on the other Dewar benzene derivatives. The effects of reactant and quencher (MPB) concentrations on DETX-sensitized isomerization of DB3 in ethyl acetate are similar to those of DB2, with Φ_{isom} leveling off at ~120 in the absence of MPB, suggesting similar propagation rate constants for DB3 and DB2. As mentioned above, the adiabatic isomerization rate constant for DB3 is also similar to that for DB2 (~4×10^9 vs ~9×10^9 s^{-1}).

For hexamethyl Dewar benzene, DB1, a high-energy sensitizer is needed due to its higher triplet energy. Xanthone derivatives, such as PXN, are not suited for prolonged irradiations, because a side reaction causes bleaching of the sensitizer. Instead 4-methoxyacetophenone (E_T = 70.9 kcal/mol, Φ_{isc} = 0.95[21]) was used. Chain amplification is also evident in the case of DB1, but with Φ_{isom} leveling off at ~16 (see the Supporting Information for details).

Finally, as noted in section 3.3, in-cage processes can be safely ignored for the triplet chain isomerization reactions in ethyl acetate described here. However, in higher viscosity solvents in-cage processes may not be ignored, and the more general expression for the isomerization quantum yield given by eq 11 must be used (see the Supporting Information for derivation).

$$\Phi_{isom} = \Phi_{isc}\alpha\frac{\dfrac{k_{P*} + k_{P*S}[S]}{(1-\gamma\delta)} + k_{P*R}[R]}{k_{P*} + (1-\alpha)k_{P*S}[S]} \qquad (11)$$

5. Refraction Changes upon Isomerization. As mentioned in the Introduction, isomerization of Dewar benzenes brings about substantial increase in the refractive index, which serves as the basis for the construction of high-efficiency optical recording materials containing the Dewar benzenes.[12] Steady-state photolysis experiments were carried out in 100 μm cells at high (~0.3−0.4 M) reactant concentrations to better mimic the conditions used for photosensitized isomerizations in polymer films.[12] The above-mentioned, viscous solvent DOA

was used in these experiments. Deoxygenation is not easily achieved in the thin cells, but proved to be unnecessary. After a very short induction period during which dissolved oxygen (~2 mM) is consumed, the photoisomerization proceeds with high quantum yields. Most probably oxygen quenching of the triplet sensitizer, S*, and triplet product, P*, produces $^1O_2$, which then reacts with the Dewar benzene reactant, R.

The degree of conversion was monitored through the change in refractive index and was confirmed by GC analysis and by UV absorption. The Dewar benzenes DB1−DB3 show greater absorption in the ~300−340 nm region than their benzene counterparts. For example, the extinction coefficient of DB2 at 320 nm is 230 M^{-1} cm^{-1}, whereas that of B2 is near zero, and the increase in the refractive index for full isomerization of a 10% solution of DB2 in DOA is 0.0045.

Representative quantum yields of reactions sensitized with DETX (7 mM) at about 40% conversion were 40 for DB2 (0.39 M) and 95 for DB3 (0.34 M). These quantum yields tend to be somewhat lower than those reported above in ethyl acetate, possibly due to the effects of trace impurities in DOA at such high conversions. A quantum yield of ~95 was also measured for DB3 isomerization sensitized with the ketocoumarin derivative KC (E_T = 55.7 kcal/mol[21]) at both 365 and 405 nm. Comparison between these reactions in a viscous solvent and those in polymeric media will be the subject of a future paper.

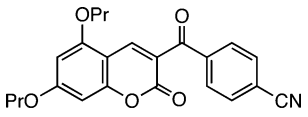

KC

Conclusions

Remarkably high isomerization quantum yields, 110−120, of Dewar benzene derivatives to the corresponding benzenes were achieved via triplet-sensitized chain reactions. These experimental values are in fact limited by trace impurities and are modeled to exceed 1000 in the absence of impurities. The release of stored energy initiated by the absorption of a photon in these systems is also considerable. For example, 436 nm photons (KC sensitizer) will lead to the release of about 106 kcal of stored energy/kcal absorbed in concentrated solutions of the diester reactant DB3 under experimental conditions. The high asymptotic quantum yields and continuing chain propagation even at high conversions are consequences of a very large adiabatic isomerization rate constant (k_a) of the triplet reactant to the triplet product (R* → P*), favorable energetics of the Dewar benzene molecules of this study, and long lifetimes of the triplet sensitizer (S*) and product (P*).

The values of k_a approaching 10^{10} s^{-1} suggest that no more than a small (~2.5−3.5 kcal/mol) energy barrier exists along the potential energy hypersurface defining the adiabatic conversion of R* to P*. Determination of these fast adiabatic rate constants relies on competition between in-cage isomerization followed by reverse energy transfer (S/R* → S/P* → S*/P) and cage separation (S/R* → S + R*) in a moderately viscous solvent. This type of analysis may prove useful for obtaining other large reaction rate constants that are difficult to directly measure.

Rate constants for energy transfer from a series of triplet sensitizers to the Dewar benzene reactants are clearly nonclassical, implying considerable distortions in the nuclear configurations between the triplet and ground states. From these experiments apparent thermodynamic triplet energies (64.5, 60, and 52.5 kcal/mol) and reorganization energies for triplet activation (3.5−4 kcal/mol) were obtained for the three Dewar benzenes used in this study (DB1, DB2, and DB3, respectively). The lower energy of the "distorted" triplet state has the beneficial effect of allowing sensitization by relatively low triplet energy sensitizers and hence the ability for excitation at wavelengths >400 nm.

The Dewar benzenes of this study have potential practical utility for optical information storage.[12] The isomerization produces a substantial increase in the refractive index that can serve as the basis for high-density, three-dimensional holographic storage of information in polymeric materials.[12] The high triplet chain isomerization quantum yields boost the efficiency of information storage, and these solution explorations aid in design optimization. The high sensitivity of the quantum yields to impurities is unlikely to play an important role in a polymeric matrix because of the highly restricted diffusion, where energy transfer is limited to nearest neighbors.

Experimental Section

Materials. Hexamethyl Dewar benzene (DB1) was obtained commercially. The syntheses of DB2 and DB3 have been described previously.[12,39,40] Ethyl acetate, tetrachloroethylene, and heptane were all 99.9% HPLC grade and were used without further purification. Bis(2-ethylhexyl) adipate (DOA) (99+%) was further purified by column chromatrography.

To ensure high photoisomerization quantum yields at high R concentrations, it is essential to use very high purity samples. DB1 (97%) was fractionally distilled from lithium aluminum hydride through a column packed with glass helices (47 °C, 17 mmHg) and was shown to be 99.8% pure by GC analysis. DB2 and DB3 were prepared as previously described,[12] and DB2 was further purified by column chromatography on silica gel (three times with 15:1 hexane/ethyl acetate as the eluent) followed by recrystallization from heptane at −78 °C and by two fractional distillations (44 °C, 0.3 mmHg). This whole purification cycle was repeated again. Purified samples were stored in a freezer to minimize thermal and oxidative degradation. Nevertheless, it proved very difficult to reduce and maintain impurity levels below about ~0.1%.

Commercially available sensitizers were purified by column chromatography and repeated recrystallization, 2,4-diethyl-9*H*-thioxanthen-9-one (DETX) from heptane, thioxanthen-9-one (TX) from methanol, and 4-methoxyacetophenone (MAP) from hexane. 2-*tert*-Pentylxanthone (PXN) and other xanthone and thioxanthone-type triplet energy donors used for energy-transfer measurements were prepared and purified as previously described.[12] Ketocoumarin sensitizer/donors, including 3-(4′-cyanobenzoyl)-5,7-dipropoxycoumarin (KC), were also prepared and purified as described previously.[41] Methyl 1-pyrenebutyrate (MPB) was prepared by esterification of commercially available 1-pyrenebutyric acid. 1,4-Dibromonaphthalene (DBN) and 1-methylphenanthrene (1MP) were recrystallized from ethanol.

Quantum Yield Measurements. Steady-state photolysis experiments were carried out under yellow lights. Sample solutions of R and the appropriate sensitizer in ethyl acetate were freshly prepared and transferred to 1.0 cm quartz cuvettes equipped with J. Young (Scientific Glassware Ltd.) high-vacuum stopcocks (slightly modified to allow straight insertion of needles) that carried serum caps. The solutions were then deoxygenated by bubbling argon for about 10 min through long syringe needles inserted through rubber septa. Some irradiations were also carried out on concentrated samples in 100 μm demountable quartz cells (Hellma Cells, Inc.) without deoxygenation.

Irradiation of sample solutions was performed on an optical bench consisting of an Oriel 6285 500 W Hg lamp (with an Oriel 68910 500 W arc lamp power supply) in an Oriel 66902 research lamp housing connected to a manual shutter, a deionized water filter, and a flanged holder containing a frosted quartz diffusing element (Edmund Industrial Optics). Pairs of filters were used to select a single mercury line: a Schott GG-395 long-pass cutoff filter followed by an Oriel 56541 interference filter for 405 nm irradiations, a Schott WG-360 long-pass cutoff filter followed by an Oriel 56531 interference filter for 365 nm irradiations, or a Schott WG-335 long-pass cutoff filter followed by an Oriel 56521 interference filter for 334 nm irradiations. UV−vis absorption spectra of sample solutions were recorded before and after irradiation on a Hewlett-Packard 8452A diode array spectrophotometer.

For actinometry, 9,10-phenanthrenequinone and 0.1 M *trans*-stilbene in benzene[42] were used for 405 nm irradiations, and ~5 mM Aberchrome 540 in toluene[43] was used at 334 nm. An EG&G 450-1 radiometer calibrated vs a standard thermopile and with Reinecke's salt actonimetry[44] was also used to monitor photon flux. Irradiated solutions were analyzed either by GC using an Agilent Technologies 6890N series gas chromatograph with an Agilent Technologies 7683 series autosampler and injector and a Hewlett-Packard Ultra-2 (5% phenyl/methyl polysiloxane) capillary column (9.6 m × 0.25 mm × 0.32 mm thickness) or by HPLC using an Agilent Technologies model 1100 series system equipped with a 1100 diode array detector and a YMC ODS-AQ 120A (100 mm × 3.0 mm × 5 mm) reversed-phase column. To determine the number molecules or moles of product formed by photolysis, aliquots of each solution were taken at various irradiation times and diluted with ethyl acetate containing an internal standard (*n*-tetradecane for GC and di-*n*-butyl phthalate for HPLC). Peaks of reactants and products referenced to internal standard were corrected with detector response factors. In thin cells, isomerization was followed via GC, UV absorption changes, and refractive index changes.

Intersystem crossing quantum yields (Φ_{isc}) for various sensitizers were measured by following the sensitized isomerization of *trans*-stilbene[45] using GC analysis and/or by measuring the intensity of T−T absorption of an appropriate triplet energy acceptor (e.g., naphthalene) produced by laser flash (vide infra) excitation of the sensitizer/donor.[46] In both cases, benzophenone ($\Phi_{isc} = 1.0$) was used as a reference.

Laser Flash Photolysis Experiments. Quenching rate constants and excited-state decay and equilibria were measured using a nanosecond laser flash photolysis apparatus described previously.[47] A Lambda Physik Lextra 50 XeCl excimer laser was used for direct sample excitation at 308 nm or to pump a Lambda Physik 3002 dye laser, providing approximately 7 ns high-intensity pulses. Most experiments described herein were carried out with 343 nm light obtained with *p*-terphenyl as the laser dye. Transient absorptions were monitored at 90° to the laser excitation using pulsed xenon lamps (Oriel 66005, 150 W for kinetics), timing shutters, a monochromator, and a photomultiplier tube for kinetic measurements or a diode array detector (Oriel Instaspec V gated and intensified CCD) for obtaining transient absorption spectra and optical densities. For kinetic analyses the signal from the photomultiplier tube was directed into a Tektronix TDS 620 digitizing oscilloscope and then to a computer for viewing, storage, and analysis. Filters were used to attenuate laser intensities to minimize ground-state depletion, photochemical reactions, light absorption byproducts, and triplet−triplet annihilation. Typically, attenuated beam energies were less than 0.2 mJ per pulse, and data were averaged over approximately 20 pulses. Excessive averaging was avoided to minimize isomerization of the reactants. For most measurements, samples in sealed 1 cm quartz cells were deoxygenated by argon bubbling.

Thermodynamic triplet energies were determined for all sensitizers used either to initiate R isomerizations or as triplet energy donors for the determination of DB triplet energies. The thermodynamic energies were measured as described previously by Kira and Thomas.[22] Experimental details and extensive data for triplet energy donors and acceptors will be provided in a subsequent paper.[21] Rate constants, k_q, for quenching of triplet sensitizers (donors) by triplet energy transfer to R acceptors were measured using sensitizer concentrations as low as possible, to minimize reverse energy transfer. Low laser pulse energies were particularly important in kinetic experiments designed to probe the quasi-equilibria among S*, R*, and P* to minimize R depletion and triplet−triplet annihilation. For these experiments initial concentrations of S* of $\leq 4 \times 10^{-6}$ M were produced by single laser pulses with thorough mixing between each of about 20 averaged pulses.

The radical cations of B1−B3, which absorb in the 460−490 nm range, were generated by electron-transfer reaction using *N*-methylquinolinium hexafluorophosphate as a photooxidant.[48] No absorptions in this wavelength range could be detected in the reactions of DB1−DB3 with DETX as the sensitizer.

Luminescence Measurements. Triplet-state energies of the benzene derivatives of this study were measured in ethyl acetate or distilled hexane at 77 K using a Fluorolog-3 spectrofluorometer (Jobin Yvon, Horiba).

Acknowledgment. Research support was provided by the National Science Foundation (Grants CHE-9812719 and DMR-0071302). We thank Mark Mis of Eastman Kodak Co. for providing many of the chemical samples used in this study, Dr. Ralph Young of the Eastman Kodak Company for valuable assistance in the kinetic fitting procedures, and Dr. Marcel Madaras of Eastman Kodak Co. for measuring electrochemical potentials.

Supporting Information Available: (I) Derivation of the Φ_{isom} expression, eq 5, (II) energetics of energy transfer to the Dewar benzenes, (III) comparative quenching in ethyl acetate and DOA, (IV) derivation of the Φ_{isom} expression including the cage term, eq 11, (V) transient kinetic data for quasi-equilibrium between DETX* and B2*, and (VI) quantum yield for triplet chain isomerization of DB1. This material is available free of charge via the Internet at http://pubs.acs.org.

References and Notes

(1) (a) Gillmore, J. G.; Neiser, J. D.; McManus, K. A.; Roh, Y.; Dombrowski, G. W.; Brown, T. G.; Dinnocenzo, J. P.; Farid, S.; Robello, D. R. *Macromolecules* **2005**, *38*, 7684. (b) Dinnocenzo, J. P.; Farid, S. Y.; Robello, D. R.; Erdogan, T. U.S. Patent 6,569,600, 2003.

(2) Renner, C. A.; Katz, T. J.; Pouliquen, J.; Turro, N. J.; Waddell, W. H. *J. Am. Chem. Soc.* **1975**, *97*, 2568.

(3) Turro, N. J.; Ramamurthy, V.; Katz, T. J. *Nouv. J. Chem.* **1977**, *1*, 363.

(4) (a) Arai, T.; Tokumaru, K. *Chem. Rev.* **1993**, *93*, 23. (b) Tokumaru, K.; Arai, T. *Bull. Chem. Soc. Jpn.* **1995**, *68*, 1065 and references therein.

(5) Okamoto, H.; Arai, T.; Sakuragi, H.; Tokumaru, K. *Bull. Chem. Soc. Jpn.* **1990**, *63*, 2881.

(6) Karatsu, T.; Tsuchiya, M.; Arai, T.; Sakuragi, H.; Tokumaru, K. *Bull. Chem. Soc. Jpn.* **1994**, *67*, 3030.

(7) Möllerstedt, H.; Wennerström, O. *J. Photochem. Photobiol., A* **2001**, *139*, 37.

(8) Whitten, D. G.; Wildes, P. D.; DeRosier, C. A. *J. Am. Chem. Soc.* **1972**, *94*, 7811.

(9) Yee, W. A.; Hug, S. J.; Kliger, D. S. *J. Am. Chem. Soc.* **1988**, *110*, 2164.

(10) Saltiel, J.; Wang, S.; Ko, D.-H.; Gormin, D. A. *J. Phys. Chem. A* **1998**, *102*, 5383.

(11) A reported isomerization quantum yield of ~100 at low conversions for 2,4-hexadiene[11a] was attributed in subsequent studies[11b,c] to the effect of a photoactive impurity. (a) Hyndman, H. L.; Monroe, B. M.; Hammond, G. S. *J. Am. Chem. Soc.* **1969**, *91*, 2852. (b) Saltiel, J.; Townsend, D. E.; Sykes, A. *J. Am. Chem. Soc.* **1973**, *95*, 5968. (c) Saltiel, J.; Metts, L.; Wrighton, M. *J. Am. Chem. Soc.* **1969**, *91*, 5684.

(12) Farid, S. Y.; Robello, D. R.; Dinnocenzo, J. P.; Merkel, P. B.; Ferrar, L. S.; Roh, Y.; Mis, M. U.S. Patent Application 2005136357 A1, June 23, 2005.

(13) Turro, N. J.; McVey, J.; Ramamurthy, V.; Lechtken, P. *Angew. Chem., Int. Ed. Engl.* **1979**, *18*, 572.

(14) As discussed in ref 4, more complex schemes may apply for cis/trans isomerizations.

(15) See, for example: (a) Mattes, S. L.; Farid, S. In *Organic Photochemistry*; Padwa, A., Ed.; Marcel Dekker: New York, 1983; Vol. 6, p 233. (b) Lewis, F. D. In *Photoinduced Electron Transfer*; Fox, M. A., Chanon, M., Eds.; Elsevier: Amsterdam, 1988; Vol. C, p 1. (c) Bauld, N. L. *Radicals, Ion Radicals, and Triplets*; Wiley-VCH: New York, 1997. (d) Kavarnos, G. J. *Fundamentals of Photoinduced Electron Transfer*; VCH: New York, 1993. (e) Schmittel, M.; Burghart, A. *Angew. Chem., Int. Ed. Engl.* **1997**, *36*, 2550.

(16) (a) Evans, T. R.; Wake, R. W.; Sifain, M. M. *Tetrahedron Lett.* **1973**, 701. (b) Kiau, S; Liu, G.; Shukla, D.; Dinnocenzo, J. P.; Young, R. H.; Farid, S. *J. Phys. Chem. A* **2003**, *107*, 3625.

(17) Measured vs SCE in methylene chloride by Dr. M. Madaras of Eastman Kodak Co.

(18) Sandros, K. *Acta Chem. Scand.* **1964**, *18*, 2355.

(19) Balzani, V.; Bolletta, F.; Scandola, F. *J. Am. Chem. Soc.* **1980**, *102*, 2152.

(20) Balzani, V.; Bolletta, F. *J. Am. Chem. Soc.* **1978**, *100*, 7404.

(21) Merkel, P. B.; Dinnocenzo, J. P. Manuscript to be submitted for publication. Because these E_T^S values are actually free energies that include possible entropy contributions, they might more properly be designated as ΔG_T^S values, but we will use the E_T^S notation here for brevity.

(22) Kira, A.; Thomas J. K. *J. Phys. Chem.* **1974**, *78*, 196 and references therein.

(23) While differences in entropy between the triplet and ground states (ΔS) are expected to be small for the relatively rigid sensitizers used in our experiments, they may not be negligible. For example, ΔS values of approximately −0.6 to −1.2, −0.2, −1.8, and −0.8 kcal/mol may be estimated at room temperature for excitation of benzophenone,[23a,b] 4-methylbenzophenone,[23c] biphenyl,[23a] and 4-methylbiphenyl,[23c] respectively, on the basis of the effect of temperature on triplet-energy-transfer equilibria. (a) Gessner, F.; Scaiano, J. C. *J. Am. Chem. Soc.* **1985**, *107*, 7206. (b) Yamaji, M.; Okada, K.; Marciniak, B.; Shizuka, H. *Chem. Phys. Lett.* **1977**, *277*, 375. (c) Zhang, D.; Closs, G. L.; Chung, D. D.; Norris, J. R. *J. Am. Chem. Soc.* **1993**, *115*, 3670.

(24) Ethyl acetate was chosen as a solvent for several reasons. It is a reasonable model for the poly(methyl methacrylate) used in analogous experiments in polymer films. It is a better solvent for some of the materials of this study than various alkanes, and it is also less likely to participate in quenching or energy transfer than benzene or toluene.[24a] (a) Coenjarts, C.; Scaiano, J. C. *J. Am. Chem. Soc.* **2000**, *122*, 3635.

(25) This is the value of k_d calculated from the Smoluchowski equation ($k_d = 4\pi N r_{S+R} D_{S+R}/1000$) with $r_{S+R} = 5.5$ Å and $D_{S+R} = 2.9 \times 10^{-5}$ cm^2 s^{-1}, where the diffusion coefficient D_{S+R} is calculated from the Stokes−Einstein equation ($D_{S+R} = D_S + D_R = RT/6\pi\eta r_S N + RT/6\pi\eta r_R N$) with $\eta = 0.5$ cP and $r_S = r_R = 2.75$ Å.

(26) For example, the triplet energy of 2-butene is ~10 kcal/mol higher than that of dimethyl fumarate, and the triplet energy of β-methylstyrene is ~5 kcal/mol higher than that of methyl cinnamate.[26a] (a) Murov, S. L; Camichael, I.; Hug, G. L. *Handbook of Photochemistry*, 2nd ed.; Marcel Dekker: New York, 1993.

(27) Whether eq 2 is precisely applicable when $\Delta S^{\ddagger}$ is nonzero is arguable. See, for example: Saltiel, J.; Marchand, G. R.; Kirkor-Kaminska, E.; Smothers, W. K.; Mueller, W. B.; Charlton, J. L. *J. Am. Chem. Soc.* **1984**, *106*, 3144.

(28) (a) Lalevée, J.; Allonas, X.; Louërat, F.; Fouassier, J. P. *J. Phys. Chem. A* **2002**, *106*, 6702. (b) Allonas, X.; Lalevee, J.; Fouassier, J. P. *Chem. Phys.* **2003**, *290*, 257. (c) Lalevee, J.; Allonas, X.; Fouassier, J. P. *Chem. Phys. Lett.* **2005**, *401*, 483.

(29) The thermodynamic triplet energy for B2 is less accurately determined due to a small amount of absorption by photoproduct(s) in the region of the sensitizer triplet transient absorption.

(30) Quantum mechanical computations of triplet energies of benzene derivatives with bulky substituents are sparse. However, calculations on *p*-xylene suggest a quinoidal triplet conformation about 4.6 kcal/mol lower in energy than the vertical hexagonal form as well as an antiquinoidal conformation that is about 0.6 kcal/mol more stable than the hexagonal form. Buma, W. J.; van der Waals, J. H.; van Hemert, M. C. *J. Chem. Phys.* **1990**, *93*, 3746.

(31) Frank, I.; Grimme, S.; Peyerimhoff, S. D. *J. Am. Chem. Soc.* **1994**, *116*, 5949.

(32) Nordin, S. B.; Strong, R. L. *Chem. Phys. Lett.* **1968**, *2*, 429.

(33) Porter, G. B. *Theor. Chim. Acta* **1972**, *24*, 265.

(34) $k_{-d} = 3000 k_d/4\pi(r_{S+R})^3 N = 3 \times 10^{10}$ s^{-1} if $k_d = 1.3 \times 10^{10}$ M^{-1} s^{-1} and $r_{S+R} = 5.5$Å: Eigen, M. *Z. Phys. Chem.* **1954**, *1*, 176.

(35) Although both k_d and k_{-d} decrease with increasing solvent viscosity, it is generally accepted that their ratio, k_{-d}/k_d, remains constant. See ref 34 and Pilling, M. J.; Seakins, P. W. *Reaction Kinetics*; Oxford University Press: Oxford, 1995; pp 146−156.

(36) The 0−0 phosphorescence band at 77 K for DETX* occurs at about 62 kcal/mol in ethyl acetate and at about 60 kcal/mol in more polarizable chloroform.

(37) TCE was chosen as an analogue of DB2 without the complications of chain isomerization. The short lifetime of triplet TCE eliminates reverse energy transfer as is the case for R, and the rate constants for quenching of triplet 1MP are similar for TCE and DB2.

(38) Scaiano, J. C.; Leigh, W. J.; Meador, M. A.; Wagner, P. J. *J. Am. Chem. Soc.* **1985**, *107*, 5086.

(39) Dopper, J. H.; Greijdanus, B.; Oudman, D.; Wynberg, H. *Tetrahedron Lett.* **1975**, 4297.

(40) Koster, J. B.; Timmermans, G. J.; van Bekkum, H. *Synthesis* **1971**, 139.

(41) Specht, D. P.; Martic, P. A.; Farid, S. *Tetrahedron* **1982**, *38*, 1203.

(42) Brown-Wensley, K. A.; Mattes, S. L.; Farid, S. *J. Am. Chem. Soc.* **1978**, *100*, 4162.

(43) Heller, H. G.; Langan, J. R. *J. Chem. Soc., Perkin Trans. 2* **1981**, 341.

(44) Wegner, E. E.; Adamson, A. W. *J. Am. Chem. Soc.* **1966**, *88*, 394.

(45) (a) Lamola, A. A.; Hammond, G. S. *J. Chem. Phys.* **1965**, *43*, 2129. (b) Valentine, D.; Hammond, G. S. *J. Am. Chem. Soc.* **1972**, *94*, 3449.

(46) (a) Richards, J. T.; West, G.; Thomas, J. K. *J. Phys. Chem.* **1970**, *74*, 4137. (b) Scaiano, J. C.; Weldon, D.; Pliva, C. N.; Martinez, L. J. *J. Phys. Chem. A* **1998**, *102*, 6898.

(47) Shukla, D.; Liu, G.; Dinnocenzo, J. P.; Farid, S. *Can. J. Chem.* **2003**, *81*, 744.

(48) Dockery, K. P.; Dinnocenzo, J. P.; Farid, S.; Goodman, J. L.; Gould, I. R.; Todd, W. P. *J. Am. Chem. Soc.* **1997**, *119*, 1876.